Environmental Science & Technology

pubs.acs.org/est

Article

Phosphorus Speciation in Atmospherically Deposited Particulate Matter and Implications for Terrestrial Ecosystem Productivity

Peggy A. O'Day,*[,⊥] Ugwumsinachi G. Nwosu,[⊥] Morgan E. Barnes, Stephen C. Hart, Asmeret Asefaw Berhe, John N. Christensen, and Kenneth H. Williams

Cite This: https://dx.doi.org/10.1021/acs.est.9b06150

Read Online

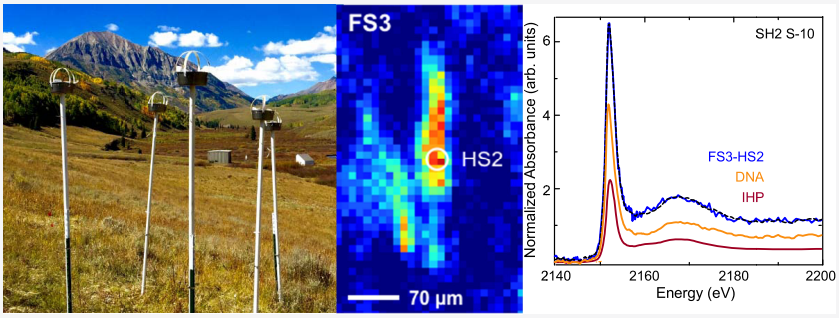

ABSTRACT: Chemical forms of phosphorus (P) in airborne particulate matter (PM) are poorly known and do not correlate with solubility or extraction measurements commonly used to infer speciation. We used P X-ray absorption near-edge structure (XANES) and ^{31}P nuclear magnetic resonance (NMR) spectroscopies to determine P species in PM collected at four mountain sites (Colorado and California). Organic P species dominated samples from high elevations, with organic P estimated at 65−100% of total P in bulk samples by XANES and 79−88% in extracted fractions (62−84% of total P) by NMR regardless of particle size (≥10 or 1−10 μm). Phosphorus monoester and diester organic species were dominant and present in about equal proportions, with low fractions of inorganic P species. By comparison, PM from low elevation contained mixtures of organic and inorganic P, with organic P estimated at 30−60% of total P. Intercontinental PM transport determined from radiogenic lead (Pb) isotopes varied from 0 to 59% (mean 37%) Asian-sourced Pb at high elevation, whereas stronger regional PM inputs were found at low elevation. Airborne flux of bioavailable P to high-elevation ecosystems may be twice as high as estimated by global models, which will disproportionately affect net primary productivity.

INTRODUCTION

Humans have profoundly altered the biogeochemical cycling of phosphorus (P) on earth through fossil fuel burning, intensive mining of mineral phosphate deposits, and widespread agricultural fertilization.[1] Recent studies have established that total P flux from deposition of airborne particulate matter (PM) can constitute a significant P source to ecosystem nutrient budgets in temperate climates,[2,3] following on prior work that documented the importance of airborne P deposition to tropical ecosystems.[4−6] The impact of nutrient deposition, particularly P, from regional and intercontinental sources on the trophic status of historically oligotrophic alpine lakes has been recognized.[7,8] Global climate models suggest that net primary productivity (NPP) may increase from carbon dioxide fertilization over the next century, resulting in net increases in carbon (C) storage in terrestrial ecosystems.[9] However, these potential productivity increases are dependent on the availability of growth-limiting nutrients such as nitrogen (N) and P, and nutrient limitation is one of the most uncertain factors in model prediction of terrestrial carbon storage under global change.[10]

Airborne PM (also referred to as aerosols) is a mixture of particles in a solid or liquid form derived from biogenic, geogenic, and anthropogenic sources. The amount and composition of PM deposited at a given location are a mixture derived from regional and intercontinental sources that vary temporally and spatially, and particles may experience acidic alteration or surface modifications (e.g., adsorbents or coatings) during atmospheric transport.[11,12] Prior studies have emphasized the importance of both natural and anthropogenic sources of atmospheric P to biogeochemical cycles.[8,13−19] Global estimates of airborne P emission and

Received: October 11, 2019
Revised: January 16, 2020
Accepted: March 17, 2020
Published: March 17, 2020

deposition fluxes are usually based on average concentrations measured in PM and differing assumptions about organic or inorganic P fractions, and their solubility, in model particle size bins.[8,13,17,19,20] Early studies concluded that atmospheric P on a global scale was dominated by inorganic P as mineral particles,[13,21] with biogenic and combustion sources comprising a relatively small fraction (<20%).[13,22] More recent estimates of global P emissions suggested increases in natural and anthropogenic combustion sources and soluble mineral dust relative to preindustrial levels,[8,19,20] and another study suggested that half of the P emitted from combustion sources may be in organic forms.[17] Most interpretations of P speciation in airborne samples are derived from measurements of total P compared with operationally defined, multistep sequential chemical extractions designed to assess P solubility or lability in different media, and thus indirectly, potential bioavailability.[23−25] While chemical extraction methods provide information about the solubility of P-bearing species, they are not necessarily definitive regarding the chemical form or bonding environment (i.e., speciation) of P in PM, and they may introduce chemical alteration or artifacts.[26] Few studies have employed direct characterization methods to identify and quantify P species in PM. Thus, there is considerable uncertainty underlying global and regional estimates of P flux regarding the form, potential bioavailability, and impact on ecosystem P cycling of aerially deposited PM.

Prior work examining P chemical speciation in airborne PM samples has been limited because of the analytical challenges associated with small sample mass, low P concentration, and small particle sizes. Synchrotron X-ray absorption spectroscopy (XAS) at the P K edge, mostly as X-ray absorption near-edge structure (XANES) analysis, has been used in a few studies to characterize P speciation in PM, with estimates of the relative proportions of organic and inorganic P in component mixtures varying from 0 to 100% by bulk P XANES fits.[27,28] In the western U.S., P XANES was used to estimate Ca−P, Fe−P, and organic P fractions in particles deposited on snow from sites in the central Rocky Mountains.[26] Particle size analysis indicated that samples were primarily silt-sized (3.9−63 μm) and dominated by Ca−P and Fe−P species (68−92%), leading the authors to conclude that the particles originated from regional sources in the Colorado plateau.[26] In PM samples deposited in volcanic areas in northern Arizona, organic P estimated by P XANES comprised from 0 to 25% of total P.[29] To our knowledge, ^{31}P NMR spectroscopy has not been applied to the study of airborne PM, although this method has been used to characterize P species in a variety of soils and environmental samples.[30,31]

We propose that the ecosystem impact of P from aerially deposited PM from global and regional sources depends on both the amount deposited and on P chemical speciation, which determines the mechanism and rate of P cycling once PM is incorporated into surface soils. In this study, we used XAS and NMR to identify P species and quantify mixtures in PM collected by passive sampling and filtration at two mountain watershed sites in Colorado (CO) and California (CA), over an approximately one year period. Potential sources of PM were evaluated using analysis of lead (Pb) isotope ratios (in particular ^{206}Pb/^{207}Pb and ^{208}Pb/^{207}Pb) and compared with a large published data set from the western United States and Asia. Lead can be emitted as a co-pollutant in industrial and urban plumes, and transported as fine aerosols, with the principal Pb fraction from 2001 to 2009 associated with coal combustion followed by nonferrous ore smelting.[32] Changes in fuel use, agricultural practices, and climate change will influence local and long-range PM sources and transport, which in turn will impact P speciation and its ability to stimulate NPP, particularly in P-limited, high-elevation ecosystems.

MATERIALS AND METHODS

See the Supporting Information (SI) for method details.

Study Sites and Sample Collection. Airborne particulate matter (PM) was collected by passive sampling at two high-elevation sites (3100 m, site LS; 2800 m, site PH) in the East River Watershed, Colorado (CO-ERW) study area, and at high- (2500−2700 m, site SH) and low (400 m, site SJ)-elevation sites in the Southern Sierra Critical Zone Observatory (CA-SSCZO; see Figure S1 and Table S1 for locations and elevations). The CO-ERW sites were sampled by dry deposition (Sept−Oct 2016) and by snow sampling (winter, 2017), and the CA-SSCZO high-elevation site was sampled twice by dry deposition (Sept−Nov. 2016; July−Sept 2017) and once by snow sampling (winter, 2017). The low-elevation site CA-SSCZO (SJ) was below the snow line and was sampled three times by dry deposition (Sept−Oct 2016; June−July 2017; Aug 2017). Samples were collected using acid-cleaned passive collectors (25.4 cm diameter Teflon-coated pans) filled with glass beads following previously employed methods.[2] Multiple collectors were deployed on 2 m high wooden poles at each site for 1−3 months. Pans were retrieved, washed with DI water, and filtered in series with 10 μm (PM $\geq$ 10 μm) and 1 μm (PM 1−10 μm) polytetrafluoroethylene (PTFE) filters (for one sample, SJ1, 0.2 μm filters were used). For snow samples, melted snow water was filtered with 10 and 1 μm PTFE filters.

Sample Analysis. *Elemental Analysis.* Elemental sample composition was determined by acid digestion of PM samples and analysis by inductively coupled plasma-optical emission spectrometry (ICP-OES; PerkinElmer Optima 5300 DV) and inductively coupled plasma-mass spectrometry (ICP-MS; Agilent 7500cs). Samples were digested using a microwave acid digestion procedure (Anton Paar Multiwave 3000) with aqua regia (9 mL HCl and 3 mL HNO_3 to ∼10−20 mg of the dried sample). Digests were diluted with ultrapure water to 4% nitric acid prior to element analysis. In addition to PM analysis, the DI water used for size filtration of PM samples was measured for dissolved total P (Figures S2 and S3).

Phosphorus K Edge XAS. Sized-fractioned PM samples were analyzed directly on filters by bulk and microfocused XANES at beamline 14-3 at the Stanford Synchrotron Radiation Lightsource (SSRL, Stanford, CA) and at the soft X-ray microcharacterization beamline (SXRMB) at the Canadian Light Source (CLS, Saskatoon, Canada). Spectra were collected by mounting PM filters on P-free, double-sided carbon tape. Samples were maintained in either a He gas environment or a vacuum during data collection at room temperature. The energy at the P K edge was calibrated using multiple standards. A set of reference spectra consisting of 17 compounds or adsorbed species was used in least-squares linear combination fits (LCF) to estimate P speciation in bulk samples (Figures S4 and S5). Standards were collected for each data collection run and cross-calibrated between different beamlines and runs. Fits were performed with the component sum not forced to unity and only best fits within 2.5% of 100% were accepted. Microfocused X-ray fluorescence (μ-XRF)

https://dx.doi.org/10.1021/acs.est.9b06150
Environ. Sci. Technol. XXXX, XXX, XXX−XXX

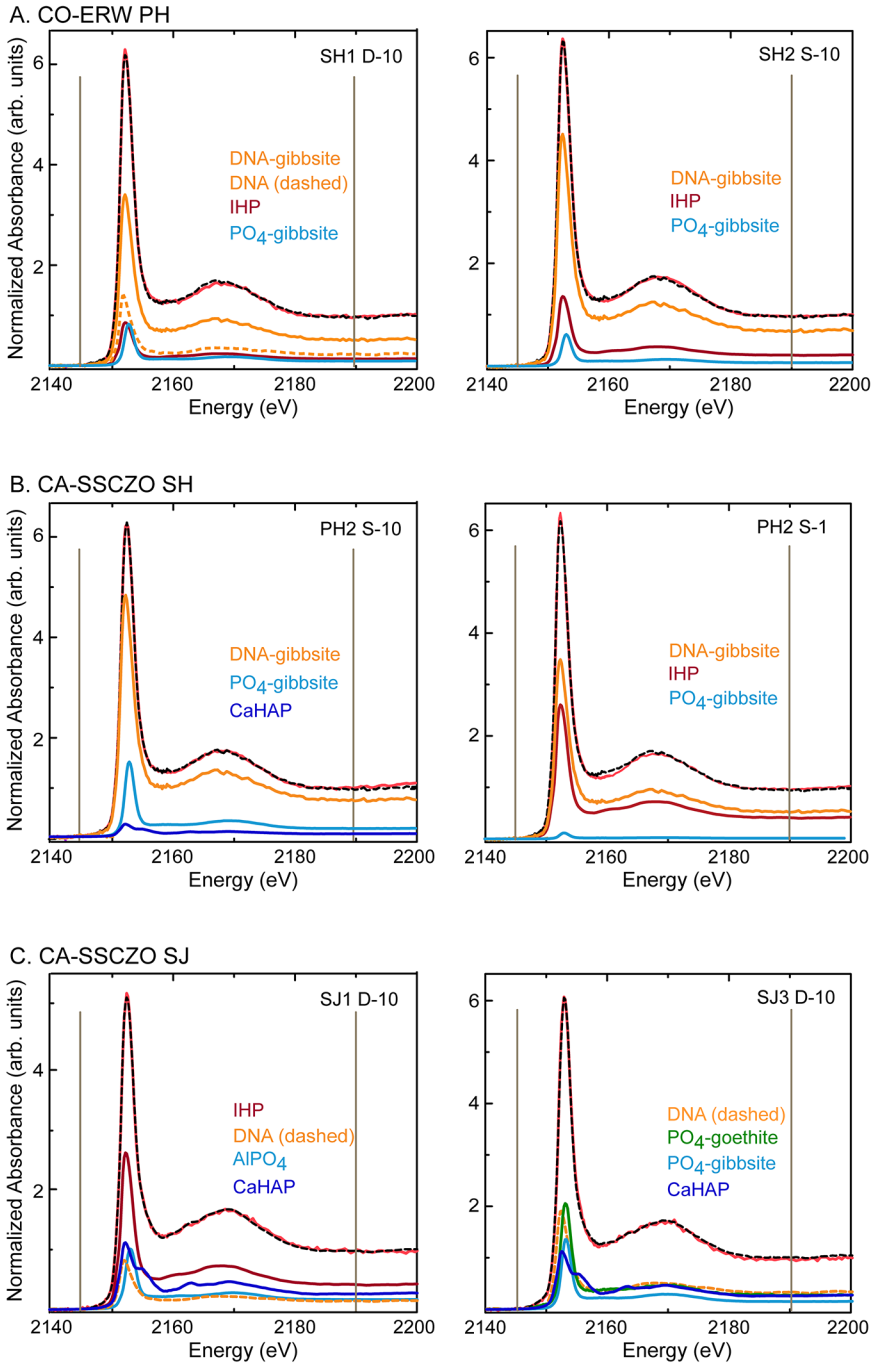

Figure 1. Phosphorus K edge XANES of bulk particulate matter samples showing data (solid red line), linear combination best fit (dashed black line), and spectral deconvolutions of reference compounds (colored lines). (A) High-elevation CO samples (PH site) comparing size fractions (10 and 1 μm filters); (B) high-elevation CA samples (SH site) comparing dry (D) and snow (S) samples (10 μm filters); (C) low-elevation CA samples (SJ site) comparing annual differences (Sept−Oct 2016 and Aug 2017; 10 μm filters). Reference spectra: inositol hexakisphosphate, Na salt (IHP); deoxyribonucleic acid (DNA); and DNA adsorbed on gibbsite (DNA-gibbsite); Ca hydroxyapatite (CaHAP), PO_4 adsorbed on gibbsite ($Al(OH)_3$; PO_4-gibbsite), and PO_4 adsorbed on goethite (FeOOH; PO_4-goethite).

maps and XANES were collected on a subset of samples using an ∼10 μm beam size to verify P components in mixtures.

Solution ^{31}P NMR. Extractable P from PM samples was characterized by solution NMR. Sample masses of 30−70 mg were extracted with 5 mL of 0.25 M NaOH and 0.05 M ethylenediaminetetraacetic acid (EDTA) solution for 6 h, followed by centrifugation. Supernatant solutions were decanted, filtered, frozen (−18 °C), and lyophilized for 24 h to concentrate extracted compounds. Freeze-dried particles were reconstituted to a 0.8−1.0 mL volume with 1 M NaOH, from which samples were prepared and immediately used for analysis by ^{31}P solution NMR. Spectra were acquired at 20 °C on a two-channel Agilent 500 MHz ProPulse500 NMR System with a One NMR Probe and a 96-Sample Robot, which operates at ^{31}P frequency of 202.4 MHz. Spectra were collected for 16 h (8600 scans), but scans were saved every 4 h (8600 scans) to monitor peaks over time. The instrument was continuously checked with an external standard (85%

https://dx.doi.org/10.1021/acs.est.9b06150
Environ. Sci. Technol. XXXX, XXX, XXX−XXX

phosphoric acid, 0 ppm) to correct for instrumental drift. Standards (sodium phosphate, D-glucose 6-phosphate, lecithin, deoxyribonucleic acid (DNA), and myo-inositol hexaphosphate (myo-IHP)) were collected individually and used to verify peak positions and chemical shifts.[31] Spectra were processed with reference to the orthophosphate peak standardized to 6 ppm.[31,33] Peak assignments were further confirmed by spiking previously analyzed samples with orthophosphate and P standards α- and β-glycerophosphate, myo-IHP, D-glucose 1-phosphate, and D-glucose 6-phosphate (Figure S6). The residue remaining after NaOH−EDTA extraction was digested and analyzed by ICP-OES to determine the amount of unextracted P by difference.

Lead Isotopic Analysis. Lead isotopic analysis was done with a Neptune Plus (Thermo-Fisher) multicollector ICP source mass spectrometer (MCICPMS) at the Lawrence Berkeley National Laboratory (LBNL) following prior methods.[34,35] Aliquots of solutions were taken from samples dissolved for total element analysis to provide 10−100 ng of Pb for isotopic analysis. Matrix elements were removed from the sample solution, which was then dried and resuspended in 1 mL of high-purity 0.3 M HNO_3, from which 10% by volume was taken for determination of Pb concentration. Based on this result, the remaining sample was spiked with natural Tl (NIST SRM997) at ∼5 ng Tl per 25 ng sample Pb. The isotopic composition of the Tl-sample Pb mixture was measured on the Neptune Plus using the monitored $^{230}Tl/^{205}Tl$ ratio to correct measured $^{206}Pb/^{207}Pb$ and $^{208}Pb/^{206}Pb$ for instrumental mass fractionation, along with normalization to the NIST SRM981 Pb isotopic standard spiked with Tl as above. Samples $^{206}Pb/^{207}Pb$ and $^{208}Pb/^{206}Pb$ were also corrected for total chemistry blank, which in most cases was less than 1% of sample Pb mass. Analytical uncertainties (2σ) of the $^{206}Pb/^{207}Pb$ and $^{208}Pb/^{206}Pb$ ratios were better than ±0.01‰ based on replicates of SRM981. The fraction of Pb in PM from Asian sources was calculated using a mixing model presented by Ewing et al.[34] and subsequent studies (Figure S7).[35−37]

RESULTS

Elemental Analysis. Bulk elemental analysis of PM showed that CO-ERW samples on average had lower P concentrations compared to those from CA-SSCZO, but there was considerable variability among samples (average P ± S.D.: 30.7 ± 9.4 vs 53.1± 19 μmol g_{PM}^{-1} or 0.951 ± 0.29 vs 1.64 ± 0.59 mg g_{PM}^{-1}, respectively; see the SI for results). The high-elevation CA-SSCZO samples (SH site) had the highest total P concentrations (mean 66.1 ± 15 μmol g_{PM}^{-1} or 2.05 ± 0.46 mg g_{PM}^{-1}), with no differences among samples collected by either dry deposition or as snow. Among the low-elevation CA-SSCZO samples, average P concentrations were lower in SJ1 and SJ3, collected in Sept−Oct 2016 and Aug 2017, respectively, compared to SJ2, collected in June−July 2017. These concentrations are similar to average values reported previously for CA-SSCZO sites.[2] Analysis of filtrate water for total P showed concentrations ranging from below instrumental detection (0.32 μmol L^{-1} or 10 μg L^{-1}) up to 65 μg L^{-1}, except for filtrate water from two low-elevation CA-SSCZO samples (SJ2 and SJ3), which contained 103.1 ± 1.2 and 327.6 ± 39.4 μg L^{-1} P, respectively. These analyses indicated that most inorganic P in PM samples was not readily water soluble over the duration of the sample filtration. Analyses of major elements showed that aluminum (Al) was the most abundant element among all samples, with the highest concentrations measured at the low-elevation SJ site, all of which were collected by dry deposition (Figure S2). Samples at the high-elevation sites were collected by either dry deposition or snow sampling, and total element concentrations were generally lower than those for SJ samples (Figures S2 and S3).

Phosphorus K Edge XANES. *Bulk XANES Spectra.* Estimates of P speciation in bulk PM samples from LCF of XANES reference spectra showed that high-elevation CO and CA sites were dominated by organic forms of P rather than inorganic P (Figures 1 and 2). At these sites, organic P

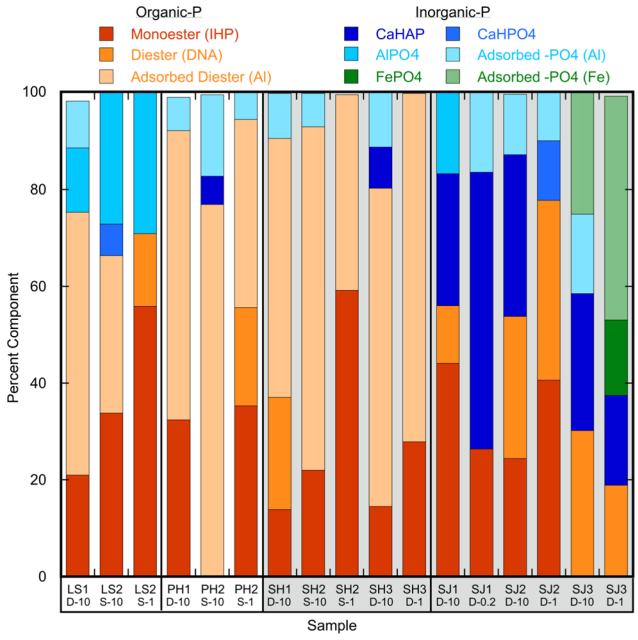

Figure 2. Summary of linear combination fits of phosphorus K edge XANES spectra of bulk particulate matter samples using reference compound spectra (component sum not normalized; see the SI for analysis details). Sites: LS, PH—high-elevation CO-ERW; SH—high-elevation CA-SSCZO; SJ—low-elevation CA-SSCZO. Sample types: D—dry; S—snow. Filter size: 10, 1, or 0.2 μm. Numerical fit results for bulk XANES spectra are reported in Table S2.

compounds, primarily as P monoesters (fit as inositol hexakisphosphate, IHP) and P diesters (fit as DNA or DNA adsorbed on gibbsite) species, comprised 66−100% of the XANES spectrum (see Table S2 for the numerical results). Inorganic Ca-phosphate (as either hydroxyapatite or $CaHPO_4$), Al-phosphate (as $AlPO_4$), or adsorbed orthophosphate (as PO_4 adsorbed on gibbsite) comprised the remaining fraction(s). At the high-elevation sites, no systematic differences were apparent among PM samples collected during summer and fall by dry deposition compared to PM filtered from melted snow samples (Figure 1). Proportions of P monoester to P diester were variable across seasons and among high-elevation sites. Hydroxyapatite (CaHAP) was detected as a minor component in only two of the samples from high-elevation sites (PH2 and SH3, ≥10 μm). Both PM ≥10 μm and PM 1−10 μm filter samples had similar components in variable mixtures, with no obvious differences (Figures 1 and 2).

Phosphorus speciation at the low-elevation CA-SSCZO site (SJ) was more variable than at high-elevation sites based on XANES fits (Figure 2). All three dry deposition samples

https://dx.doi.org/10.1021/acs.est.9b06150
Environ. Sci. Technol. XXXX, XXX, XXX−XXX

contained different proportions of organic and inorganic forms of P, the latter varying from 22 to 81% of total P. All spectra contained Ca-phosphate (as CaHAP; one spectrum had $CaHPO_4$) and often a fraction of Al-phosphate (as $AlPO_4$ or PO_4 sorbed on gibbsite). Samples collected over one summer month (SJ3, Aug 2017) were notable for containing a significant fraction of inorganic Fe-phosphate species (as orthophosphate sorbed on goethite or $FePO_4$) in addition to Ca-phosphate (Figure S5). Organic P species were a mixture of P monoesters (as IHP) and P diesters (as DNA).

Microfocused (μ-)XRF and XANES. The spatial distribution and speciation of P were studied in selected PM samples (≥10 μm; LS2, SH2, and SJ2) using μ-XRF and μ-XANES to examine heterogeneity and compare with bulk XANES analysis. Fluorescence mapping showed that P was distributed sparsely in PM samples with a few spots of concentrated P. In general, μ-XANES spectra collected at hot spots were mixtures of more than one P species at the scale of the beam spot (10 μm), with components similar to those identified in the bulk spectrum. Analysis of μ-XANES from the CO-ERW LS site showed evidence for P monoester and diester components either as bulk or adsorbed species, and a minor amount of inorganic P fit as adsorbed orthophosphate (Figure 3a). Similarly, P hot spots in the high-elevation CA-SSCZO (SH2) were dominated by organic P, with minor inorganic P species (Figure 3b). Consistent with the analysis of bulk XANES spectra of the low-elevation CA-SSCZO SJ site, μ-XANES spectra of hot spots in the SJ2 sample were more variable and showed mixtures of organic and inorganic P species (Figure 3c). Some μ-XANES spectra from SJ showed features characteristic of mineral hydroxyapatite, whereas other μ-XANES spectra were fit with mixtures of P monoester and P diester spectra.

Solution ^{31}P NMR Analysis of Extracted PM Samples. A subset of samples (≥10 μm) were extracted by NaOH–EDTA solutions and analyzed by ^{31}P solution NMR (Figure 4). The fraction of total P extracted to solution was higher in samples from high-elevation CO-ERW and CA-SSCZO sites (80–89%) than from the low-elevation CA-SSCZO SJ site (51%; Table 1). Spectra from the high-elevation LS and SH sites exhibited a higher abundance of peaks associated with organic P monoester and dieseter compounds than the low-elevation SJ site (Figure 4). Inorganic and organic P fractions determined by area integration of chemical shift peaks identified in the NMR spectra and summation of chemical classes (Table S3) showed that all of the high-elevation sites were dominated by organic P compounds (66–78%). The low-elevation SJ site was the only site in which the fraction of inorganic P (68%) was greater than that of organic P (Table 1). The diester region of the NMR spectrum was composed primarily of DNA (~−0.3 ppm), but there was also evidence of peaks assignable to RNA, phospholipids (PL), lipoteichoic acids (LTA), and their degradation products (Figure 4; Table S3).[31] Peaks in the P monoester region indicated the presence of IHP, α- and β-glycerophosphate, and sugar phosphates (D-glucose 1-phosphate and D-glucose 6-phosphate) (Figure S6). Among inorganic P species, spectra were dominated by orthophosphate, and minor peaks were assigned to pyrophosphate, doublet polyphosphates end groups, and triplet polyphosphate midchain groups (Table S3). Inorganic polyphosphate groups contributed about 5–10% of the extractable P in all samples.

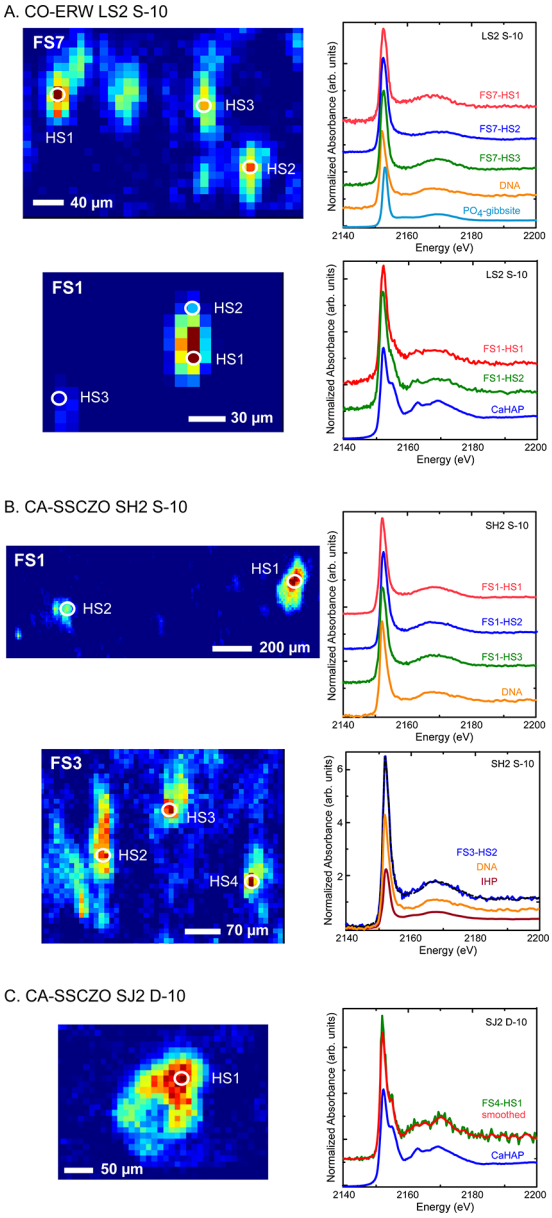

Figure 3. Representative phosphorus K edge μ-XRF maps and μ-XANES (spot size ~10 μm) of airborne particles on filters compared with reference spectra deoxyribonucleic acid (DNA), PO_4 adsorbed on gibbsite (PO_4-gibbsite), and Ca hydroxyapatite (CaHAP). (A) High-elevation CO sample LS2 S-10; (B) high-elevation CA sample SH2 S-10; linear combination fit (in black) of two reference spectra (DNA and inositol hexakisphosphate, IHP) shown for hot spot 2 (HS2); (C) low-elevation CA sample SJ2 D-10; raw (green) and smoothed (red) spectra compared with reference spectrum Ca hydroxyapatite (CaHAP).

Summation of chemical shift peak areas showed that P monoester compounds were more abundant overall than P diester compounds. However, monoester α- and β-glycerophosphate are thought to be degradation products of primary phospholipid compounds generated during chemical extraction and NMR analysis.[38,39] Correcting for this degradation from diester to monoester compounds shifted ratios such that P diester compounds were about twice as abundant as P monoesters at the high-elevation sites, whereas monoester P compounds were still more abundant at the low-elevation SJ site (Table 1).

https://dx.doi.org/10.1021/acs.est.9b06150
Environ. Sci. Technol. XXXX, XXX, XXX−XXX

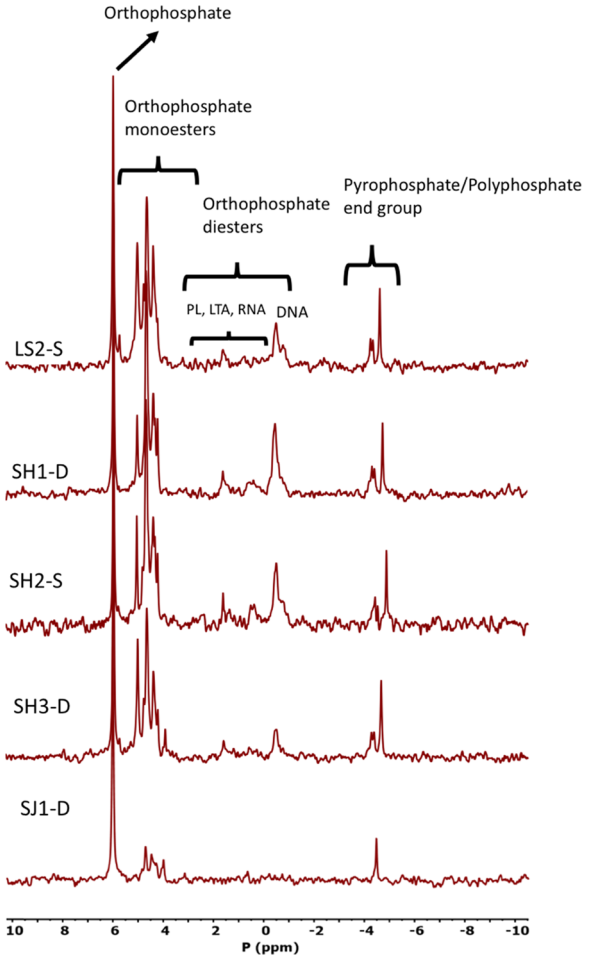

Figure 4. ^{31}P solution NMR spectra of extracted PM from high-elevation CO (LS2-S) and CA (SH1-D, SH2-S, SH3-D) sites compared with the low-elevation CA site (SJ1-D). PL: phospholipids; LTA: lipoteichoic acid; RNA: ribonucleic acid; and DNA: deoxyribonucleic acid. See Table 1 for estimates of relative fractions of P species from peak area integration and Table S3 for peak assignments.

Pb Isotope Analysis. Ratios of naturally occurring isotopes of lead (^{206}Pb, ^{207}Pb, and ^{208}Pb) in samples were measured to estimate sources of PM following prior studies of Pb fingerprinting of PM2.5 samples in the western U.S.[34−37] The measured ^{206}Pb/^{207}Pb and ^{208}Pb/^{206}Pb of the PM samples (Figure 5) were used to calculate the fraction of Pb in the sample originating from Asian sources using the mixing model of Ewing et al.[34] (see Table S4 and Figure S7). In general,

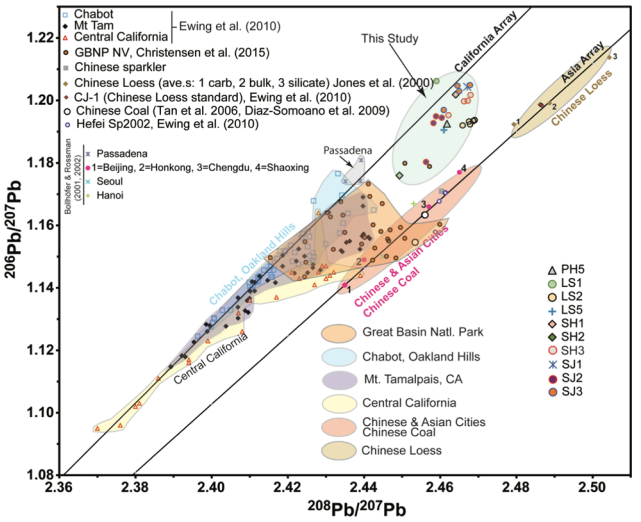

Figure 5. Lead (Pb) isotope ratios of particulate matter samples (from individual filters) compared with samples from prior studies of airborne particles from the western U.S. and sources in China. This study: LS, PH—high-elevation CO-ERW; SH—high-elevation CA-SSCZO; SJ—low-elevation CA-SSCZO. Published studies: Ewing et al.;[34] Christensen et al.;[35] Jones et al.;[40] Tan et al.;[41] and Diaz-Somoano et al.[42] See Table S4 for the numerical results.

^{206}Pb/^{207}Pb and ^{208}Pb/^{206}Pb of this study were higher than those measured in prior studies of PM samples from central California and eastern Nevada (Figure 5). Mixing calculations showed variable inputs of Pb from Asian sources ranging from 0 to 59% among all samples, with some samples collected at the same time having similar Pb isotope ratios and others not (Table S4 and Figure S8). For example, isotope ratios of replicate filters (n = 5) of melted snow from CO-ERW (LS2) were tightly clustered, with the fraction of Asian Pb varying from 52 to 59%. In dry deposition samples collected in fall 2016 (LS1, PH1), the fraction of Asian Pb was lower (0−34%). Analyses of replicate filter samples (dry deposition, n = 4) in fall 2017 from high-elevation CA-SSCZO (SH3) had similar fractions of Asian Pb (26−31%), whereas a snowmelt sample (SH2) had lower ^{206}Pb/^{207}Pb and ^{208}Pb/^{206}Pb ratios and a higher Asian Pb fraction (38%). Analyses of dry deposition samples from low-elevation CA-SSCZO (SJ1, SJ2, and SJ3) had variable amounts of Asian Pb, even among replicate filter samples (Figure 5 and Table S4). For example, Asian Pb in SJ2 replicates (n = 4) varied from 14 to 52%, whereas SJ3 replicates (n = 4) varied from 5 to 17% Asian Pb. However, Pb concentrations were also variable among replicates; for example, SJ2 replicates ranged in Pb

Table 1. Percentage of Total Extracted Phosphorus (P) from NaOH−EDTA Extraction and Proportion of P Species in Extracted Solutions Estimated from Integration and Correction of NMR Peaks

sample[a]	extracted P[b] (% of total)	inorganic P (%)	organic P (%)	monoester (%)	diester (%)	monoester/diester	monoester[c] (corrected %)	diester[c] (corrected %)	monoester/diester (corrected)
LS2-S	80	25.4	74.6	60.2	14.4	4.2	27.3	47.3	0.58
SH1-D	85	26.4	73.6	53.3	20.3	2.6	22.6	51.0	0.44
SH2-S	89	22.3	77.7	57.7	20.0	2.9	27.9	49.8	0.56
SH3-D	89	33.5	66.5	56.1	10.4	5.4	19.4	47.1	0.41
SJ1-D	51	67.7	32.3	31.1	1.20	26	21.3	11.0	1.9

[a]Samples composited from multiple 10 μm filters to obtain 30−70 mg of dry mass; D: dry, S: snow. [b]Determined by digestion of the total sample and residue after NaOH−EDTA extraction and analysis of total P by ICP-OES. [c]Estimated fractions corrected for degradation of diester phospholipid compounds to monoester α- and β-glycerophosphate.

https://dx.doi.org/10.1021/acs.est.9b06150
Environ. Sci. Technol. XXXX, XXX, XXX−XXX

concentration from 24 to 33 ppm, with the highest concentration corresponding to the highest faction of Asian Pb (Table S4). Overall, the high-elevation sites (CO and CA) had a mean estimated Asian Pb fraction of 36.8% (n = 14), while the mean from low-elevation (CA) samples was 19.3% (n = 9).

DISCUSSION

Phosphorus Speciation in Deposited Particulate Matter. Spectroscopic characterization of PM samples by two independent methods, synchrotron XAS and solution ^{31}P NMR, showed that P speciation in samples from high-elevation sites in CO and CA was dominated by organic P species, regardless of season or PM size (either ≥10 μm or between 1 and 10 μm). In contrast, the low-elevation CA site had variable mixtures of different organic and inorganic P species. These results demonstrate that P in airborne PM is a spatially and temporally variable mixture of different types of P compounds that is not dominated by inorganic orthophosphate compounds or species, and reflects input from local, regional, and intercontinental sources (see below). Bulk XANES analysis performed directly on sample filters produced a weighted distribution of all P species in a sample, while NMR analysis provided detailed identification of P species in the base-extractable fraction. The fraction of organic P was estimated at 66−100% from P XANES and species identification was corroborated by microfocused mapping and XANES spectral analysis. The fraction of total P removed by chemical extraction (62−84%) in high-elevation samples was mostly organic P, as determined by NMR (79−88%). In contrast, P species from the low-elevation CA-SSCZO SJ site contained variable mixtures of total organic (30−60% by XANES) and low total extractable (51%) P that was mostly inorganic P (65%), as indicated by NMR. Samples from the SJ site had the highest fractions of crystalline P phases by XANES (fit as hydroxyapatite or $CaHPO_4$) and high fractions of adsorbed and Fe-associated orthophosphate over all periods of sample collection. Although temporal sampling was limited to about one year, no obvious differences were apparent among samples at high-elevation sites collected by dry deposition over one to two months during the fall compared with melted snow samples collected at the end of winter and integrated over a longer deposition period. For all samples, PM was suspended in aqueous solution (either by washing pans or melting snow) and filtered, so any highly soluble compounds were dissolved, and the remaining less soluble material would represent particles that would be delivered to the surface soil. Comparison of the speciation and extraction results indicates that organic P and adsorbed orthophosphate were more readily extracted by NaOH−EDTA than crystalline P phases, and that most organic P was extracted from bulk samples by this chemical treatment. These results agree with a prior study of PM samples using P XANES and extraction that noted a higher solubility in general for organic P compared with inorganic P fractions, but also emphasized variability among samples and poor correlation of extractable P with XANES component assignments.[27]

Estimates of the distribution of organic P species by XANES or NMR differed by method but were in general agreement. XANES fits estimated mostly higher fractions of P diester compared with P monoester, whereas the uncorrected NMR results indicated that organic P was present mostly as P monoester species, with a smaller fraction of P diester. Monoester species were dominated by inositol phosphates (as myo-IHP), which are produced by plants and are common in seeds and soils. Diester species were distributed mostly as DNA and RNA, which are common to all living organisms, and phospholipids, which are a major component of cell membranes.[43,44] However, correction of estimated fractions by accounting for degradation of phospholipid diester compounds to monoester α- and β-glycerophosphate indicates slightly more diester than monoester species in most high-elevation PM samples, roughly similar to the XANES results. Additional uncertainty arises from the estimation methods used for determining components in mixtures for each technique (spectral fitting for XANES; peak assignments and integrations for NMR). As discussed in prior reviews,[45−47] ^{31}P NMR spectroscopy is sensitive to chemical shifts in different organic and inorganic P species, and can provide more detail about individual species than P XANES, but characterization of bulk materials compared to sample extracts remains a challenge for NMR. For XANES, using a large set of reference spectra (n = 17) in our analysis improved the ability to differentiate types of P species between organic and inorganic classes (Figures S4 and S5). Prior P XANES studies of soil and PM samples that used few P reference compound spectra in their XANES LCF analysis may have inaccurately estimated P fractions by assuming that all organically bound forms of P had a similar spectral signature. Although different types of organically bound P are spectrally similar and lack distinct features in their XANES, our data showed subtle but resolvable differences among different classes of organic P compounds, particularly between P monoester and diester linkages and among P monoester (phytate) bonded to metal cations (see the SI), as noted in other studies.[48,49]

Sources of Phosphorus in Particulate Matter. Analysis of Pb isotopes of PM samples indicated that seasonally variable long-range transport from Asian sources is a significant contributor of PM to both CO and CA high-elevation sites in the western U.S. (up to 59% Asian Pb; mean 36.8%), but was generally lower at the low-elevation CA SJ site over all seasons (mean 19.3%; Figure S8). Samples from the SJ site collected in Aug 2017 (SJ3), which had low organic P and high fractions of inorganic Fe- and Ca-associated P determined by XANES analysis, had low Asian Pb fractions (5−17%), suggesting that these inorganic P species were locally or regionally derived from the California Central Valley to the west of the CA-SSCZO sites. Molar ratios of total P to Pb in digested PM samples varied by almost an order of magnitude (P/Pb = 127−1200), but there was no correlation of P/Pb with the Asian Pb fraction (Figure S9). Prior studies of PM sourcing using Pb isotopic ratios of PM2.5 samples found a median value of 29% Asian input to coastal California sites[34] and seasonally high inputs to California and the Great Basin in spring and fall.[34,36,37] Using Sr and Nd isotopes, Aciego et al.[2] estimated that 18−45% of PM deposited at the CA-SSCZO sites was sourced from Asia, with the remaining fraction derived regionally from the California Central Valley. At two high-elevation CA-SSCZO sites, it was estimated that about 10−20% of PM input in July was derived from Asia, whereas about 20−40% was Asian-sourced in October.[50] In the Great Basin and Colorado Plateau, regional PM sources are generally to the west-southwest, while trans-Pacific air masses often move in from the west-northwest, to episodically supply PM from a mixture of sources.[34,36,37] Prior studies estimated that, on average annually, about one-third of the PM deposited in

https://dx.doi.org/10.1021/acs.est.9b06150
Environ. Sci. Technol. XXXX, XXX, XXX−XXX

the western U.S. is sourced from the Asian continent, although inputs are spatially and temporally variable.[34,36,37] Aerosols from Asia are a mixture of anthropogenic combustion products and geogenic particles from desert regions.[36,51] Our data are in agreement with these prior studies that demonstrated a mix of Asian and local sources for PM, and similarly showed variability among samples collected over the same time interval in the fraction of PM derived from local or regional sources compared to intercontinental transport.

Previous studies of global P transport in airborne PM classified sources of P as mostly geogenic dust, biomass burning (including fossil fuels, biofuels, and wildland fires), and primary biogenic particles (e.g., vegetation, microorganisms, decomposed biomolecules), with minor inputs from industrial and mining emissions and volcanoes.[8,13,17,19,20] One prior study suggested that bacteria were a dominant source of soluble organic P in marine aerosols from the Mediterranean Sea,[27] while another estimated that half of the P emitted from combustion sources may be in organic forms.[17] We were not able to distinguish whether organic P in our samples comes from primary biogenic or fossil organic (combustion) sources, or a mixture of both. Inorganic P species have been attributed to local or regional sources of aeolian geogenic dust,[26,28] and it is likely that higher fractions of inorganic P at the SJ site reflect regional input from the Central Valley. Regarding the inorganic P fraction in our high-elevation PM samples, we observed evidence for orthophosphate adsorbed to Al- or Fe-oxide phases rather than, or in addition to, crystalline phosphate phases such hydroxyapatite. Adsorbed orthophosphate may have been derived from the breakdown of either organic compounds or primary phosphate minerals either at the source (e.g., combustion or in soil), as a result of atmospheric alteration in acidic conditions,[12,20,52] or post-depositional alteration.

Implications for Ecosystem Productivity. As an essential plant nutrient, P bioavailability can control the rate of nonagricultural, P-limited ecosystems to sequester carbon.[10] Classical models of pedogenesis hold that weathering of inorganic P in soils is a dominant source of P for biosynthesis, but in recent decades, the importance of organically bound P in ecosystem nutrient regulation has emerged.[43,44] Studies of soil and aquatic environments suggest that the most rapidly exchanging pool of P is associated with degradation of labile organic matter.[43,53] Short-term rates of organic P conversion to dissolved orthophosphate (gross mineralization) estimated from radioactive isotope dilution experiments are fast, generally in the range of 0.1−2.5 mg P kg_{soil}^{-1} day^{-1} and as high as 12.6 mg P kg_{soil}^{-1} day^{-1}, and are thought to be mostly controlled by biological and enzymatic processes.[54] For example, a key step in the conversion of organic P species to orthophosphate is the hydrolysis of the P−O−C ester linkage in P diesters and terminal P monoesters catalyzed by biologically produced phosphatase enzymes.[55,56] With soil development, some P may partition to occluded or protected pools that are relatively nonbioavailable, with decomposition rates orders of magnitude slower than fast-cycling C and nutrient pools.[57,58]

Our spectroscopic evidence showed that, regardless of particle size or season of deposition, aerially deposited PM is dominated at high-elevation sites by organic P in monoester and diester molecular forms in about equal proportions, not inorganic P in primary mineral phases such as apatite. Orthophosphate diester compounds are generally more soluble and undergo degradation by hydrolysis more readily than monoester IHP, and thus are thought to be more labile and bioavailable than IHP in the soil environment.[39,44,54,59] However, quantitative measurements of reaction rates for particular compound classes are lacking. Some studies have suggested that adsorption of organic P compounds reduces P bioavailability, but other studies argue that adsorption on mineral surfaces may promote hydrolysis and enhance bioavailability.[60−62] Phosphate apatite minerals generally have low solubilities and slow kinetic rates of dissolution that are pH-dependent,[63,64] and their bioavailability in soils will depend on factors such as particle size and surface area, degree of crystallinity, and local solution pH and cation concentration. Plants and microorganisms take up orthophosphate ($H_{3-x}PO_4^{x-}$), but since dissolved concentrations in soils are generally very low, organisms have multiple strategies for solubilizing P from both organic and inorganic pools through the secretion of organic acids, carboxylate anions, and organic metabolites.[53,65] Overall, our results suggest that, at high-elevation sites, the dominance of reactive organic P chemical species and noncrystalline inorganic P, together with small particle sizes of airborne PM, should result in P deposition that is rapidly assimilated by biological soil processes.

Recent global modeling estimates of total P emissions to the atmosphere range from about 1.3 to 3.7 Tg P $year^{-1}$,[19,20,22] but estimates of the soluble or bioavailable P fractions vary depending on model assumptions. Most models rely on a combination of factors, including size fraction distributions, bulk elemental composition, elemental ratios, and operational solubility measurements of PM, together with atmospheric transport modeling, to estimate P depositional fluxes and soluble fractions.[8,13,17] For example, Myriokefalitakis et al.[20] estimated that fractions deposited as soluble P (0.45 Tg P $year^{-1}$) or bioavailable P (0.47 Tg P $year^{-1}$) were about 35% of the total P depositional flux (1.3 Tg P $year^{-1}$), and that more than 80% of total P emissions were derived from "mineral" P sources. In contrast, Wang et al.[19] estimated a higher global total P annual emission (3.5 Tg P $year^{-1}$) based on higher P contributions (over 50%) from fossil fuel and biomass combustion sources. A recent study showed seasonally higher intercontinental transport of soluble P attributed to biomass burning from Africa to the Amazon basin as a nutrient source that may increase primary production.[25] It has been assumed that the P fraction derived from combustion sources is more soluble and thus more bioavailable in oceans[13,20] and potentially in tropical forests,[25] although other studies have shown more complicated relationships between P solubility as measured by water or chemical extractions and bioavailability.[23,66] Although our data set is limited, our determination of organic P species comprising 60−100% of total P in PM at two high-elevation sites suggests that the fraction of soluble or bioavailable P may be higher than estimated in current global cycling models (by 30−50%), and that model assumption about P speciation in particle size fractions may require reconsideration.[19,20,22]

As ecosystem NPP and organic matter cycling rates increase with climate warming, the amount and speciation of P in PM from both regional and intercontinental sources will have an increasingly important effect on P-limited ecosystems. This is particularly true for mountain regions where up-gradient shifts of vegetation zones with warming are already occurring, but changes in nutrient availability (particularly N and P) are poorly known and may constrain these vegetation range

https://dx.doi.org/10.1021/acs.est.9b06150
Environ. Sci. Technol. XXXX, XXX, XXX−XXX

shifts.[67] On both a global and regional scale, P emission fluxes to the atmosphere are likely to increase, driven by combustion of fuel and biomass, agricultural practices and land management (e.g., deforestation, grazing), increasing intensity and frequency of droughts, and other anthropogenic forcings if current trends continue.[19,25] To accurately predict impacts and design effective mitigation policies, ecosystem models will need to incorporate both total fluxes and species-based cycling rates of P into future projections. Given the P species in deposited PM identified here, we suggest that airborne P flux to high-elevation regions that is soluble or bioavailable may be twice as high as estimated by current global models. This depositional flux will have a disproportionate effect on NPP by supplying a high fraction of reactive P species that will cycle rapidly when incorporated into surface soils.

■ ASSOCIATED CONTENT

Supporting Information

The Supporting Information is available free of charge at https://pubs.acs.org/doi/10.1021/acs.est.9b06150.

Detailed descriptions of materials and methods; table of sample locations and sampling periods; figures of total element concentrations, P XANES reference spectra, chemical shift regions and standards for ^{31}P NMR spectra, illustration of the calculation for Asian Pb fraction, and percent Asian Pb as a function of site elevation and molar P/Pb; tables with fit results for bulk XANES spectra, NMR chemical shift assignments for standards, and Pb concentrations, isotope ratios, and Asian fraction (PDF)

■ AUTHOR INFORMATION

Corresponding Author

Peggy A. O'Day − *Life and Environmental Sciences Department and The Sierra Nevada Research Institute, University of California, Merced, California 95343, United States;* orcid.org/0000-0002-8698-5159; Email: poday@ucmerced.edu

Authors

Ugwumsinachi G. Nwosu − *Life and Environmental Sciences Department and The Sierra Nevada Research Institute, University of California, Merced, California 95343, United States*

Morgan E. Barnes − *Environmental Systems Graduate Group, University of California, Merced, California 95343, United States*

Stephen C. Hart − *Life and Environmental Sciences Department and The Sierra Nevada Research Institute, University of California, Merced, California 95343, United States*

Asmeret Asefaw Berhe − *Life and Environmental Sciences Department and The Sierra Nevada Research Institute, University of California, Merced, California 95343, United States*

John N. Christensen − *Earth and Environmental Sciences, Lawrence Berkeley National Laboratory, Berkeley, California 94720, United States;* orcid.org/0000-0002-9533-5801

Kenneth H. Williams − *Earth and Environmental Sciences, Lawrence Berkeley National Laboratory, Berkeley, California 94720, United States; Rocky Mountain Biological Lab, Gothic, Colorado 81225, United States*

Complete contact information is available at: https://pubs.acs.org/10.1021/acs.est.9b06150

Author Contributions

$^{\perp}$P.A.O. and U.G.N. contributed equally to this work.

Notes

The authors declare no competing financial interest.

■ ACKNOWLEDGMENTS

This research was funded by the Subsurface Biogeochemical Research Program (DE-SC0016479), U.S. Department of Energy. Portions of this research were carried out at the Stanford Synchrotron Radiation Lightsource, a national user facility operated by Stanford University on behalf of the U.S. Department of Energy, and at the Canadian Light Source, supported by the Canada Foundation for Innovation, Natural Sciences and Engineering Research Council of Canada, the University of Saskatchewan, the Government of Saskatchewan, Western Economic Diversification Canada, the National Research Council Canada, and the Canadian Institutes of Health Research. Field sample collection in Colorado and Pb isotope analyses was supported as part of the Watershed Function Scientific Focus Area at LBNL funded by the U.S. Department of Energy under Award Number DE-AC02-05CH11231. We thank Ben Lash, Erin Stacy, and Melissa Thaw for assistance at the CA-SSCZO (supported by the National Science Foundation EAR-0725097, 1239521, and 1331939) and to Dave Rice and Fernanda Santos for help with NMR analysis. Barbara Cade-Menun provided valuable advice on NMR. The UC Merced Environmental Analytical Laboratory supported analytical instrumentation.

■ REFERENCES

(1) Cordell, D.; White, S. Life's Bottleneck: Sustaining the World's Phosphorus for a Food Secure Future. In *Annual Review of Environment and Resources*; Gadgil, A.; Liverman, D. M., Eds.; Annual Reviews: Palo Alto, 2014; Vol. 39, p 161.

(2) Aciego, S. M.; Riebe, C. S.; Hart, S. C.; Blakowski, M. A.; Carey, C. J.; Aarons, S. M.; Dove, N. C.; Botthoff, J. K.; Sims, K. W. W.; Aronson, E. L. Dust outpaces bedrock in nutrient supply to montane forest ecosystems. *Nat. Commun.* **2017**, *8*, No. 14800.

(3) Arvin, L. J.; Riebe, C. S.; Aciego, S. M.; Blakowski, M. A. Global patterns of dust and bedrock nutrient supply to montane ecosystems. *Sci. Adv.* **2017**, *3*, No. eaao1588.

(4) Chadwick, O. A.; Derry, L. A.; Vitousek, P. M.; Huebert, B. J.; Hedin, L. O. Changing sources of nutrients during four million years of ecosystem development. *Nature* **1999**, *397*, 491−497.

(5) Pett-Ridge, J. C. Contributions of dust to phosphorus cycling in tropical forests of the Luquillo Mountains, Puerto Rico. *Biogeochemistry* **2009**, *94*, 63−80.

(6) Yu, H. B.; Chin, M.; Yuan, T. L.; Bian, H. S.; Remer, L. A.; Prospero, J. M.; Omar, A.; Winker, D.; Yang, Y. K.; Zhang, Y.; Zhang, Z. B.; Zhao, C. The fertilizing role of African dust in the Amazon rainforest: A first multiyear assessment based on data from Cloud-Aerosol Lidar and Infrared Pathfinder Satellite Observations. *Geophys. Res. Lett.* **2015**, *42*, 1984−1991.

(7) Homyak, P. M.; Sickman, J. O.; Melack, J. M. Pools, transformations, and sources of P in high-elevation soils: Implications for nutrient transfer to Sierra Nevada lakes. *Geoderma* **2014**, *217*−*218*, 65−73.

(8) Brahney, J.; Mahowald, N.; Ward, D. S.; Ballantyne, A. P.; Neff, J. C. Is atmospheric phosphorus pollution altering global alpine Lake stoichiometry? *Global Biogeochem. Cycles* **2015**, *29*, 1369−1383.

(9) Todd-Brown, K. E. O.; Randerson, J. T.; Hopkins, F.; Arora, V.; Hajima, T.; Jones, C.; Shevliakova, E.; Tjiputra, J.; Volodin, E.; Wu, T.; Zhang, Q.; Allison, S. D. Changes in soil organic carbon storage

predicted by Earth system models during the 21st century. *Biogeosciences* **2014**, *11*, 2341−2356.
(10) Wieder, W. R.; Cleveland, C. C.; Smith, W. K.; Todd-Brown, K. Future productivity and carbon storage limited by terrestrial nutrient availability. *Nat. Geosci.* **2015**, *8*, 441−444.
(11) Perlwitz, J. P.; Garcia-Pando, C. P.; Miller, R. L. Predicting the mineral composition of dust aerosols - Part 1: Representing key processes. *Atmos. Chem. Phys.* **2015**, *15*, 11593−11627.
(12) Stockdale, A.; Krom, M. D.; Mortimer, R. J. G.; Benning, L. G.; Carslaw, K. S.; Herbert, R. J.; Shi, Z. B.; Myriokefalitakis, S.; Kanakidou, M.; Nenes, A. Understanding the nature of atmospheric acid processing of mineral dusts in supplying bioavailable phosphorus to the oceans. *Proc. Natl. Acad. Sci. U.S.A.* **2016**, *113*, 14639−14644.
(13) Mahowald, N.; Jickells, T. D.; Baker, A. R.; Artaxo, P.; Benitez-Nelson, C. R.; Bergametti, G.; Bond, T. C.; Chen, Y.; Cohen, D. D.; Herut, B.; Kubilay, N.; Losno, R.; Luo, C.; Maenhaut, W.; McGee, K. A.; Okin, G. S.; Siefert, R. L.; Tsukuda, S. Global distribution of atmospheric phosphorus sources, concentrations and deposition rates, and anthropogenic impacts. *Global Biogeochem. Cycles* **2008**, *22*, No. GB4026.
(14) Okin, G. S.; Mahowald, N.; Chadwick, O. A.; Artaxo, P. Impact of desert dust on the biogeochemistry of phosphorus in terrestrial ecosystems. *Global Biogeochem. Cycles* **2004**, *18*, No. GB2005.
(15) Neff, J. C.; Ballantyne, A. P.; Farmer, G. L.; Mahowald, N. M.; Conroy, J. L.; Landry, C. C.; Overpeck, J. T.; Painter, T. H.; Lawrence, C. R.; Reynolds, R. L. Increasing eolian dust deposition in the western United States linked to human activity. *Nat. Geosci.* **2008**, *1*, 189−195.
(16) Mahowald, N. Aerosol Indirect Effect on Biogeochemical Cycles and Climate. *Science* **2011**, *334*, 794−796.
(17) Kanakidou, M.; Duce, R. A.; Prospero, J. M.; Baker, A. R.; Benitez-Nelson, C.; Dentener, F. J.; Hunter, K. A.; Liss, P. S.; Mahowald, N.; Okin, G. S.; Sarin, M.; Tsigaridis, K.; Uematsu, M.; Zamora, L. M.; Zhu, T. Atmospheric fluxes of organic N and P to the global ocean. *Global Biogeochem. Cycles* **2012**, *26*, No. GB3026.
(18) Boyle, J. F.; Chiverrell, R. C.; Norton, S. A.; Plater, A. J. A leaky model of long-term soil phosphorus dynamics. *Global Biogeochem. Cycles* **2013**, *27*, 516−525.
(19) Wang, R.; Balkanski, Y.; Boucher, O.; Ciais, P.; Penuelas, J.; Tao, S. Significant contribution of combustion-related emissions to the atmospheric phosphorus budget. *Nat. Geosci.* **2015**, *8*, 48−54.
(20) Myriokefalitakis, S.; Nenes, A.; Baker, A. R.; Mihalopoulos, N.; Kanakidou, M. Bioavailable atmospheric phosphorous supply to the global ocean: a 3-D global modeling study. *Biogeosciences* **2016**, *13*, 6519−6543.
(21) Graham, W. F.; Duce, R. A. Atmospheric pathways of the phosphorus cycle. *Geochim. Cosmochim. Acta* **1979**, *43*, 1195−1208.
(22) Tipping, E.; Benham, S.; Boyle, J. F.; Crow, P.; Davies, J.; Fischer, U.; Guyatt, H.; Helliwell, R.; Jackson-Blake, L.; Lawlor, A. J.; Monteith, D. T.; Rowe, E. C.; Toberman, H. Atmospheric deposition of phosphorus to land and freshwater. *Environ. Sci.: Processes Impacts* **2014**, *16*, 1608−1617.
(23) Anderson, L. D.; Faul, K. L.; Paytan, A. Phosphorus associations in aerosols: What can they tell us about P bioavailability? *Mar. Chem.* **2010**, *120*, 44−56.
(24) Gross, A.; Goren, T.; Pio, C.; Cardoso, J.; Tirosh, O.; Todd, M. C.; Rosenfeld, D.; Weiner, T.; Custodio, D.; Angert, A. Variability in Sources and Concentrations of Saharan Dust Phosphorus over the Atlantic Ocean. *Environ. Sci. Technol. Lett.* **2015**, *2*, 31−37.
(25) Barkley, A. E.; Prospero, J. M.; Mahowald, N.; Hamilton, D. S.; Popendorf, K. J.; Oehlert, A. M.; Pourmand, A.; Gatineau, A.; Panechou-Pulcherie, K.; Blackwelder, P.; Gaston, C. J. African biomass burning is a substantial source of phosphorus deposition to the Amazon, Tropical Atlantic Ocean, and Southern Ocean. *Proc. Natl. Acad. Sci. U.S.A.* **2019**, *116*, 16216−16221.
(26) Zhang, Z.; Goldstein, H. L.; Reynolds, R. L.; Hu, Y.; Wang, X.; Zhu, M. Phosphorus Speciation and Solubility in Aeolian Dust Deposited in the Interior American West. *Environ. Sci. Technol.* **2018**, *52*, 2658−2667.
(27) Longo, A. F.; Ingall, E. D.; Diaz, J. M.; Oakes, M.; King, L. E.; Nenes, A.; Mihalopoulos, N.; Violaki, K.; Avila, A.; Benitez-Nelson, C. R.; Brandes, J.; McNulty, I.; Vine, D. J. P-NEXFS analysis of aerosol phosphorus delivered to the Mediterranean Sea. *Geophys. Res. Lett.* **2014**, *41*, 4043−4049.
(28) Hudson-Edwards, K. A.; Bristow, C. S.; Cibin, G.; Mason, G.; Peacock, C. L. Solid-phase phosphorus speciation in Saharan Bodele Depression dusts and source sediments. *Chem. Geol.* **2014**, *384*, 16−26.
(29) Gu, C.; Hart, S. C.; Turner, B. L.; Hu, Y.; Meng, Y.; Zhu, M. Aeolian dust deposition and the perturbation of phosphorus transformations during long-term ecosystem development in a cool, semi-arid environment. *Geochim. Cosmochim. Acta* **2019**, *246*, 498−514.
(30) Cade-Menun, B.; Liu, C. W. Solution Phosphorus-31 Nuclear Magnetic Resonance Spectroscopy of Soils from 2005 to 2013: A Review of Sample Preparation and Experimental Parameters. *Soil Sci. Soc. Am. J.* **2014**, *78*, 19−37.
(31) Cade-Menun, B. J. Improved peak identification in P-31-NMR spectra of environmental samples with a standardized method and peak library. *Geoderma* **2015**, *257*−*258*, 102−114.
(32) Li, Q.; Cheng, H. G.; Zhou, T.; Lin, C. Y.; Guo, S. The estimated atmospheric lead emissions in China, 1990-2009. *Atmos. Environ.* **2012**, *60*, 1−8.
(33) Feng, W.; Zhu, Y.; Wu, F.; He, Z.; Zhang, C.; Giesy, J. P. Forms and Lability of Phosphorus in Algae and Aquatic Macrophytes Characterized by Solution 31P NMR Coupled with Enzymatic Hydrolysis. *Sci. Rep.* **2016**, *6*, No. 37164.
(34) Ewing, S. A.; Christensen, J. N.; Brown, S. T.; Vancuren, R. A.; Cliff, S. S.; Depaolo, D. J. Pb Isotopes as an Indicator of the Asian Contribution to Particulate Air Pollution in Urban California. *Environ. Sci. Technol.* **2010**, *44*, 8911−8916.
(35) Christensen, J. N.; Weiss-Penzias, P.; Fine, R.; McDade, C. E.; Trzepla, K.; Brown, S. T.; Gustin, M. S. Unraveling the sources of ground level ozone in the Intermountain Western United States using Pb isotopes. *Sci. Total Environ.* **2015**, *530*−*531*, 519−525.
(36) Asher, E. C.; Christensen, J. N.; Post, A.; Perry, K.; Cliff, S. S.; Zhao, Y. J.; Trousdell, J.; Faloona, I. The Transport of Asian Dust and Combustion Aerosols and Associated Ozone to North America as Observed From a Mountaintop Monitoring Site in the California Coast Range. *J. Geophys. Res.: Atmos.* **2018**, *123*, 5667−5680.
(37) Pierce, A. M.; Gustin, M. S.; Christensen, J. N.; Loria-Salazar, S. M. Use of multiple tools including lead isotopes to decipher sources of ozone and reactive mercury to urban and rural locations in Nevada, USA. *Sci. Total Environ.* **2018**, *615*, 1411−1427.
(38) Doolette, A. L.; Smernik, R. J.; Dougherty, W. J. Spiking Improved Solution Phosphorus-31 Nuclear Magnetic Resonance Identification of Soil Phosphorus Compounds. *Soil Sci. Soc. Am. J.* **2009**, *73*, 919−927.
(39) Schneider, K. D.; Cade-Menun, B. J.; Lynch, D. H.; Voroney, R. P. Soil Phosphorus Forms from Organic and Conventional Forage Fields. *Soil Sci. Soc. Am. J.* **2016**, *80*, 328−340.
(40) Jones, C. E.; Halliday, A. N.; Rea, D. K.; Owen, R. M. Eolian inputs of lead to the North Pacific. *Geochim. Cosmochim. Acta* **2000**, *64*, 1405−1416.
(41) Tan, M. G.; Zhang, G. L.; Li, X. L.; Zhang, Y. X.; Yue, W. S.; Chen, J. M.; Wang, Y. S.; Li, A. G.; Li, Y.; Zhang, Y. M.; Shan, Z. C. Comprehensive study of lead pollution in Shanghai by multiple techniques. *Anal. Chem.* **2006**, *78*, 8044−8050.
(42) Diaz-Somoano, M.; Kylander, M. E.; Lopez-Anton, M. A.; Suarez-Ruiz, I.; Martinez-Tarazona, M. R.; Ferrat, M.; Kober, B.; Weiss, D. J. Stable Lead Isotope Compositions In Selected Coals From Around The World And Implications For Present Day Aerosol Source Tracing. *Environ. Sci. Technol.* **2009**, *43*, 1078−1085.
(43) Baldwin, D. S. Organic phosphorus in the aquatic environment. *Environ. Chem.* **2013**, *10*, 439−454.
(44) Condron, L. M.; Turner, B. L.; Cade-Menun, B. J. Chemistry and Dynamics of Soil Organic Phosphorus. In *Phosphorus: Agriculture and the Environment*;Sims, J. T.; Sharpley, A. N., Eds.; Agronomy

https://dx.doi.org/10.1021/acs.est.9b06150
Environ. Sci. Technol. XXXX, XXX, XXX−XXX

Monograph 46; ASA, CSSA, and SSSA: Madison, WI, 2005; pp 87−121.
(45) Cade-Menun, B. J. Using Phosphorus-31 Nuclear Magnetic Resonance Spectroscopy to Characterize Organic Phosphorus in Environmental Samples. In *Organic Phosphorus in the Environment*; Turner, B. L.; Frossard, E.; Baldwin, D. S., Eds.; CABI Publishing: Wallingford, Oxon, GBR, 2004; pp 21−44.
(46) Cade-Menun, B. J. Characterizing phosphorus in environmental and agricultural samples by P-31 nuclear magnetic resonance spectroscopy. *Talanta* **2005**, *66*, 359−371.
(47) Doolette, A. L.; Smernik, R. J. Soil Organic Phosphorus Speciation Using Spectroscopic Techniques. In *Phosphorus in Action: Biological Processes in Soil Phosphorus Cycling*; Bunemann, E. K.; Oberson, A.; Frossard, E., Eds.; Springer-Verlag: Berlin, Heidelberg, 2011; Vol. *26*, pp 3−36.
(48) Hesterberg, D. Macroscale Chemical Properties and X-Ray Absorption Spectroscopy of Soil Phosphorus. In *Developments in Soil Science*; Balwant, S.; Markus, G., Eds.; Elsevier, 2010; Chapter 11, Vol. *34*, pp 313−356.
(49) Prietzel, J.; Harrington, G.; Hausler, W.; Heister, K.; Werner, F.; Klysubun, W. Reference spectra of important adsorbed organic and inorganic phosphate binding forms for soil P speciation using synchrotron-based K-edge XANES spectroscopy. *J. Synchrotron Radiat.* **2016**, *23*, 532−544.
(50) Aarons, S. M.; Arvin, L. J.; Aciego, S. M.; Riebe, C. S.; Johnson, K. R.; Blakowski, M. A.; Koornneef, J. M.; Hart, S. C.; Barnes, M. E.; Dove, N.; Botthoff, J. K.; Maltz, M.; Aronson, E. L. Competing droughts affect dust delivery to Sierra Nevada. *Aeolian Res.* **2019**, *41*, No. 100545.
(51) Brock, C. A.; Hudson, P. K.; Lovejoy, E. R.; Sullivan, A.; Nowak, J. B.; Huey, L. G.; Cooper, O. R.; Cziczo, D. J.; de Gouw, J.; Fehsenfeld, F. C.; Holloway, J. S.; Hubler, G.; Lafleur, B. G.; Murphy, D. M.; Neuman, J. A.; Nicks, D. K.; Orsini, D. A.; Parrish, D. D.; Ryerson, T. B.; Tanner, D. J.; Warneke, C.; Weber, R. J.; Wilson, J. C. Particle characteristics following cloud-modified transport from Asia to North America. *J. Geophys. Res.: Atmos.* **2004**, *109*, No. D23S26.
(52) Nenes, A.; Krom, M. D.; Mihalopoulos, N.; Van Cappellen, P.; Shi, Z.; Bougiatioti, A.; Zarmpas, P.; Herut, B. Atmospheric acidification of mineral aerosols: a source of bioavailable phosphorus for the oceans. *Atmos. Chem. Phys.* **2011**, *11*, 6265−6272.
(53) Jansa, J.; Finlay, R.; Wallander, H.; Smith, F. A.; Smith, S. E. Role of Mycorrhizal Symbioses in Phosphorus Cycling. In *Phosphorus in Action: Biological Processes in Soil Phosphorus Cycling*; Bunemann, E. K.; Oberson, A.; Frossard, E., Eds.; Springer-Verlag: Berlin, Heidelberg, 2011; Vol. *26*, pp 137−168.
(54) Bünemann, E. K. Assessment of gross and net mineralization rates of soil organic phosphorus - A review. *Soil Biol. Biochem.* **2015**, *89*, 82−98.
(55) Quiquampoix, H.; Mousain, D. Enzymatic Hydrolysis of Organic Phosphorus. In *Organic Phosphorus in the Environment*; Turner, B. L.; Frossard, E.; Baldwin, D. S., Eds.; CABI Publishing: Wallingford, Oxon, GBR, 2004; pp 89−112.
(56) Nannipieri, P.; Giagnoni, L.; Landi, L.; Renella, G. Role of Phosphatase Enzymes in Soil. In *Phosphorus in Action: Biological Processes in Soil Phosphorus Cycling*; Bunemann, E. K.; Oberson, A.; Frossard, E., Eds.; Springer-Verlag: Berlin, Heidelberg, 2011; Vol. *26*, pp 215−243.
(57) Parton, W. J.; Stewart, J. W. B.; Cole, C. V. Dynamics of C, N, P and S in grassland soils: a model. *Biogeochemistry* **1988**, *5*, 109−131.
(58) Fatichi, S.; Manzoni, S.; Or, D.; Paschalis, A. A Mechanistic Model of Microbially Mediated Soil Biogeochemical Processes: A Reality Check. *Global Biogeochem. Cycles* **2019**, *33*, 620−648.
(59) Darch, T.; Blackwell, M. S. A.; Hawkins, J. M. B.; Haygarth, P. M.; Chadwick, D. A Meta-Analysis of Organic and Inorganic Phosphorus in Organic Fertilizers, Soils, and Water: Implications for Water Quality. *Crit. Rev. Environ. Sci. Technol.* **2014**, *44*, 2172−2202.
(60) Olsson, R.; Giesler, R.; Loring, J. S.; Persson, P. Adsorption, Desorption, and Surface-Promoted Hydrolysis of Glucose-1-Phosphate in Aqueous Goethite (alpha-FeOOH) Suspensions. *Langmuir* **2010**, *26*, 18760−18770.
(61) Olsson, R.; Giesler, R.; Loring, J. S.; Persson, P. Enzymatic Hydrolysis of Organic Phosphates Adsorbed on Mineral Surfaces. *Environ. Sci. Technol.* **2012**, *46*, 285−291.
(62) Baldwin, D. S.; Howitt, J. A.; Beattie, J. K. Abiotic Degradation of Organic Phosphorus Compounds in the Environment. In *Organic Phosphorus in the Environment*;Turner, B. L.; Frossard, E.; Baldwin, D. S., Eds.; CABI Publishing: Wallingford, Oxon, GBR, 2004; pp 75−88.
(63) Drouet, C. A comprehensive guide to experimental and predicted thermodynamic properties of phosphate apatite minerals in view of applicative purposes. *J. Chem. Thermodyn.* **2015**, *81*, 143−159.
(64) Oelkers, E. H.; Valsami-Jones, E.; Roncal-Herrero, T. Phosphate mineral reactivity: from global cycles to sustainable development. *Mineral. Mag.* **2008**, *72*, 337−340.
(65) Jones, D. L.; Oburger, E. Solubilization of Phosphorus by Soil Microorganisms. In *Phosphorus in Action: Biological Processes in Soil Phosphorus Cycling*; Bunemann, E. K.; Oberson, A.; Frossard, E., Eds.; Springer-Verlag: Berlin, Heidelberg, 2011; Vol. *26*, pp 169−198.
(66) Li, B.; Brett, M. T. The influence of dissolved phosphorus molecular form on recalcitrance and bioavailability. *Environ. Pollut.* **2013**, *182*, 37−44.
(67) Hagedorn, F.; Gavazov, K.; Alexander, J. M. Above- and belowground linkages shape responses of mountain vegetation to climate change. *Science* **2019**, *365*, 1119.

https://dx.doi.org/10.1021/acs.est.9b06150
Environ. Sci. Technol. XXXX, XXX, XXX−XXX